Voltage controlled spin injection in a (Ga,Mn)As/(Al,Ga)As Zener diode

P. Van Dorpe, W. Van Roy, J. De Boeck, and G. Borghs
IMEC, Kapeldreef 75, B-3001 Leuven, Belgium

P. Sankowski and P. Kacman
Institute of Physics, Polish Academy of Sciences, al. Lotników 32/46, 02-668 Warszawa, Poland

J.A. Majewski
Institute of Theoretical Physics, Warsaw University, ul. Hoża 69, 00-681 Warszawa, Poland

T. Dietl
Institute of Physics, Polish Academy of Sciences and ERATO Semiconductor Spintronics Project, al. Lotników 32/46, 02-668 Warszawa, Poland
Institute of Theoretical Physics, Warsaw University, ul. Hoża 69, 00-681 Warszawa, Poland
(Dated: March 23, 2024)

The spin polarization of the electron current in a p-(Ga,Mn)As-n-(Al,Ga)As-Zener tunnel diode, which is embedded in a light-emitting diode, has been studied theoretically. A series of self-consistent simulations determines the charge distribution, the band bending, and the current-voltage characteristics for the entire structure. An empirical tight-binding model, together with the Landauer-Büttiker theory of coherent transport has been developed to study the current spin polarization. This dual approach allows to explain the experimentally observed high magnitude and strong bias dependence of the current spin polarization.

PACS numbers: 75.50.Pp, 72.25.Hg, 73.40.Gk

Spin injection is one of the target applications of ferromagnetic semiconductors, which can serve as a natural supply of highly spin-polarized carriers. In particular, the most intensively studied ferromagnetic semiconductor (Ga,Mn)As can be grown epitaxially on GaAs and the carrier-mediated ferromagnetism in this material provides an elegant way to control the ferromagnetic properties by tuning the hole concentration.[1] In the design of spintronic devices, the p-type character of (Ga,Mn)As introduces a disadvantage due the low hole spin lifetimes in GaAs. It has been shown that interband (Zener) tunneling from valence band electrons of (Ga,Mn)As to the conduction band of GaAs is a way to circumvent this disadvantage.[2,3] Recently, an injected spin polarization up to 80% at 4.6 K has been demonstrated in a (Ga,Mn)As based spin-light emitting diode (LED) using Zener tunneling.[4] Moreover, the degree of injected spin polarization exhibits a strong dependence on the applied bias. The spin polarization reaches its maximum just above the electroluminescence threshold and decreases dramatically at higher bias. This effect is very interesting for spintronic applications, since it provides a manner to control the degree of injected spin polarization with the applied voltage.

In this Rapid Communication, we analyze theoretically the transport in the spin-LED as a function of the applied bias by means of self-consistent simulations. Furthermore, we compute the degree of current spin polarization at the (Ga,Mn)As/GaAs-interface by combining an empirical tight-binding model with the Landauer-Büttiker theory of coherent transport. We show that the decrease of the polarization with bias is caused by an increased electron tunneling from the valence band of depleted (Ga,Mn)As and non-magnetic GaAs. This offers the opportunity to tune the spin current polarization by an external electric field.

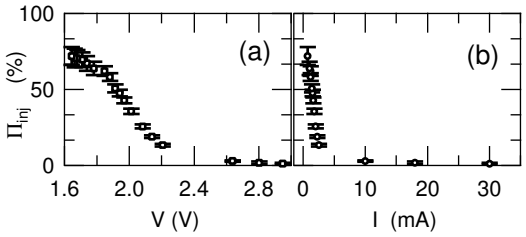

FIG. 1: The degree of injected spin polarization measured at 4.6 K as a function of the applied bias voltage (a) and the current (b) from Ref. 4.

The device considered here has the following structure: p^+ GaAs substrate / 200 nm p-$Al_{0.3}Ga_{0.7}As$ ($2 \cdot 10^{18}$ cm^{-3}) / 100 nm p-GaAs ($2 \cdot 10^{18}$ cm^{-3}) / 60 nm n-$Al_xGa_{1-x}As$ ($1 \cdot 10^{17}$ cm^{-3}) / 30 nm n-$Al_xGa_{1-x}As$ ($1 \cdot 10^{18}$cm^{-3}) / 9 nm n-GaAs ($9 \cdot 10^{18}$cm^{-3}) / 20 nm $Ga_{0.92}Mn_{0.08}As$, i.e., the spin-LED from Ref. 4. In this structure, the Al-concentration in the spin-drift region is engineered together with the doping concentration in order to provide an effective barrier for the holes, such that carrier generation due to impact ionization is eliminated at low bias. The measured[4] spin polarization is shown as a function of the applied bias voltage and current in Fig. 1(a) and 1(b), respectively. The spin polarization decreases dramatically with increasing bias.

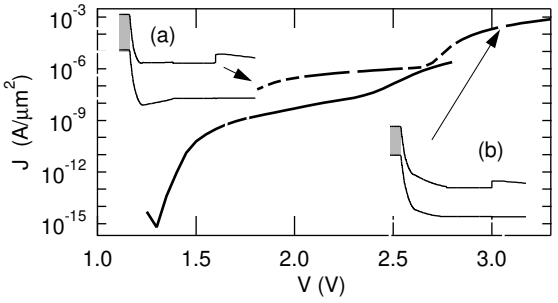

FIG. 2: The measured current (solid line) at 4.6 K as a function of the applied bias voltage (Ref. 4) and the simulated current (dashed line) as a function of the applied bias voltage. The insets show the simulated conduction and valence band profiles at (a) 1.8 and (b) 3.0 V bias. The grey-colored area represents the (Ga,Mn)As injector.

We first model the charge transport in the device by means of a series of self-consistent simulations of the entire LED under bias using Medici,[5] a semiconductor simulation tool that allows self-consistent calculations of semiconductor heterostructures taking into account band-to-band tunneling, recombination and impact ionization. In these simulations the (Ga,Mn)As region is treated as a heavily doped GaAs region. The value of the doping level is chosen based on transport measurements on samples grown using similar growth conditions on a semi-insulating substrate. In the self-consistent simulations, the interband tunneling is taken into account using the Kane model to introduce a generation term.[6] In the simulations, the generation of carriers due to interband tunneling is calculated assuming a completely filled valence band. Due to the large Fermi energy (E_F) in (Ga,Mn)As, the carriers depart from E_F below the valence band maximum. This results in a small error in the bias voltage where interband tunneling takes place, but does not qualitatively alter the results of the calculations. Impact ionization is treated in a post-processing mode, i.e., the carrier generation is calculated after the self-consistent calculation of the band bending. For comparison, the simulated current density at 40 K is shown together with the measured current density at 5 K as a function of the applied bias voltage on Fig. 2. Due to well-known numerical convergence issues, we have been unable to simulate the structure at 5 K. There is a good qualitative agreement between the simulated and the measured behavior, taking into account that the doping levels and aluminum concentrations used in the simulations are nominal and can differ from reality. Between 1.6 V and 2.3–2.5 V the current is dominated by interband tunneling of electrons through the (Ga,Mn)As/GaAs tunnel diode, while above 2.6 V the current is dominated by the holes, which can freely flow from the substrate to the top contact. Figure 3 shows the band diagram (solid lines) of the (Ga,Mn)As–(Al,Ga)As diode together with the Al concentration and the carrier generation due to interband tunneling (filled black) as a function of the depth near the (Ga,Mn)As/GaAs-interface at 1.8 V and at 3 V. There are two peaks present in the plotted carrier generation, one in the (Ga,Mn)As-area, which shows the generated holes in the (Ga,Mn)As valence band, and one in the GaAs area that shows the generated electrons in the GaAs conduction band. From this picture we can deduce that interband tunneling takes place from the valence band of (Ga,Mn)As to the conduction band of GaAs. When GaAs changes into (Al,Ga)As, the increasing Al concentration causes a widening of the band gap and an abrupt increase of the tunneling distance. This results in an exponentially smaller tunneling probability and hence the number of electrons that is generated in the (Al,Ga)As region is negligible. This means that only the part of the (Ga,Mn)As valence band that overlaps with the GaAs conduction band can participate in the tunneling process. If we compare the low and the high bias case we see that the area from where electrons tunnel (the left peak in the carrier generation) is much bigger at high bias than at low bias. When the voltage drop over the tunnel diode increases, the part of the valence band of (Ga,Mn)As that aligns with the conduction band of GaAs increases and hence the tunneling originates from a wider region. In Fig. 4 we show the hole concentration and the (normalized) carrier generation due to interband tunneling as a function of the depth near the (Ga,Mn)As-GaAs interface for different values of

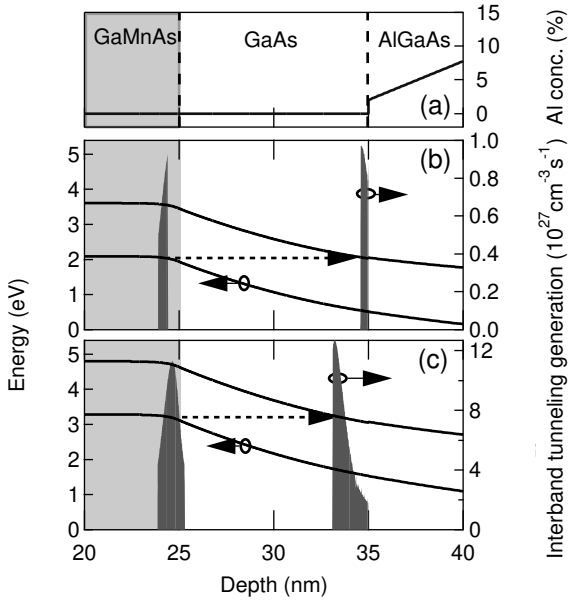

FIG. 3: The Al concentration (solid line) (a), the band diagram (solid lines) and the carrier generation (filled) due to interband tunneling (dotted line) as a function of the depth near the (Ga,Mn)As/GaAs tunnel diode at 1.8 V (b) and 3 V (c). The grey-coloured area represents the (Ga,Mn)As injector. The dotted arrows indicate the tunneling of valence electrons from (Ga,Mn)As to GaAs.

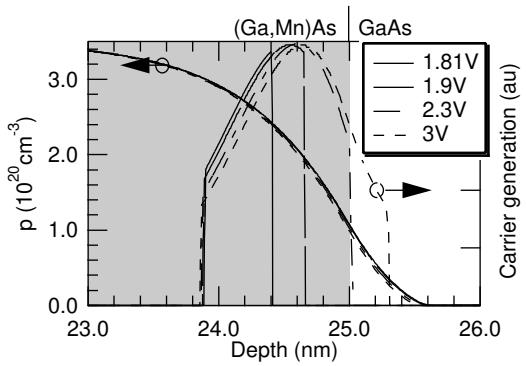

FIG. 4: The hole concentration (left) and the carrier generation due to interband tunneling (right) at different values of the applied bias voltage near the (Ga,Mn)As/GaAs interface. The grey-coloured area represents the (Ga,Mn)As injector.

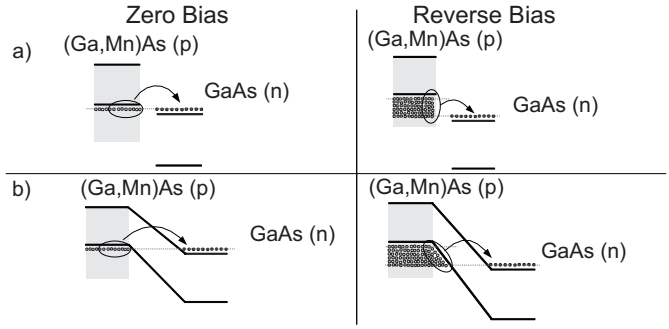

FIG. 5: Scheme of the structure used in the tight-binding calculations, at zero and at reverse bias without (a) and with the GaAs spacer (b).

the applied bias voltage. The simulations show that the hole concentration decreases in the bottom two nanometer of the (Ga,Mn)As-layer due to the band bending in the (Ga,Mn)As-GaAs p-n-diode. Increasing the voltage has a negligible influence on the hole depletion near the interface. However, we do see a big change in the properties of the tunneling region. At low bias, the tunneling electrons mainly depart from a region where the hole concentration is smaller than, but close to the bulk value, while at higher bias this region shifts and widens such that electrons can tunnel from a region where the hole concentration is much lower. At a somewhat higher bias (> 2.2V) we see that also electrons from the valence band of the non-magnetic GaAs layer participate in the tunneling process. In the experiment this bias will probably be lower due to the above described small error in the interband tunneling model.

Apart from Zener tunneling, also impact ionization can contribute to the generation of electrons in the GaAs conduction band. This process generates unpolarized electron-hole pairs and hence dilutes the injected spins and diminishes the measured spin polarization. Impact ionization in this case is caused by holes that flow from the substrate to the top contact and are heavily accelerated by the strong electric field near the (Ga,Mn)As-GaAs interface. However, the simulations indicate that the carrier generation due to impact ionization only starts dominating at the (second) hump in the IV-characteristics, where the valence band reaches a flatband-situation (Fig. 2, inset (b)) and the holes can flow freely from the substrate to the top contact. Below this "hump" impact ionization can be neglected.

In parallel to self-consistent calculations that allow a detailed understanding of the charge distribution, band bending, electron and hole currents and their bias dependence, in order to study the current spin polarization, we have developed a model of interband tunneling, which combines an empirical tight-binding approach with the Landauer-Buttiker formalism.[8] To describe the band structure of GaAs we use the $sp^3d^5s^*$ tight-binding parametrization, with the spin-orbit coupling included, proposed by Jancu et al.[9] This model reproduces correctly the effective masses and the band structure of GaAs in the whole Brillouin zone, in agreement with the results obtained by empirically corrected pseudopotential method. The presence of Mn ions in GaMnAs is taken into account by including the sp-d exchange interactions within the virtual crystal and mean-field approximations, with the values of the exchange constants determined by the observed spin splittings of the conduction and valence bands. Importantly, in contrast to the standard $k \cdot p$ method, our model takes automatically into account the Rashba and Dresselhaus terms, and is therefore particularly well suited to describe interface phenomena such as tunneling.

Because of computational constraints in approaches involving transfer matrix formalism,[8] carrier transport along the whole device cannot be simulated. Therefore, we consider first the simplest p-$Ga_{1-x}Mn_xAs$/n-GaAs tunneling structure shown in Fig. 5(a). Guided by previous theories of tunneling magnetoresistance (TMR), we expect that while such model overestimates necessarily the tunneling current, it can provide quantitative information on current spin polarization that is determined by inter-band tunneling matrix elements and degree of spin polarization in the ferromagnetic electrode.

In our computation, we assume that the magnetization vector is by 27° out of plane, as implied by experimental conditions.[4] We evaluate the spin current polarization P_j in respect to this direction. Furthermore, we estimate that for a T_c of 120 K and $x = 0.08$, the expected hole concentration is of the order of $p = 3.5 \cdot 10^{20}$ cm^{-3}, as indicated by the experimental results in Ref. 10. We also assume that the electron concentration is $n = 10^{19}$ cm^{-3}. The dependence of P_j on the hole concentration p is depicted in Fig. 6. Previous calculations have shown that the spin polarization of the hole liquid decreases with p in $Ga_{1-x}Mn_xAs$.[7] In this case, P_j, the spin polarization of the tunneling electrons, shows a similar behavior as function of p. This is naturally caused by the fact that in the relevant range of p and x, $Ga_{1-x}Mn_xAs$ is not half-metallic, so that the Fermi energy is greater than

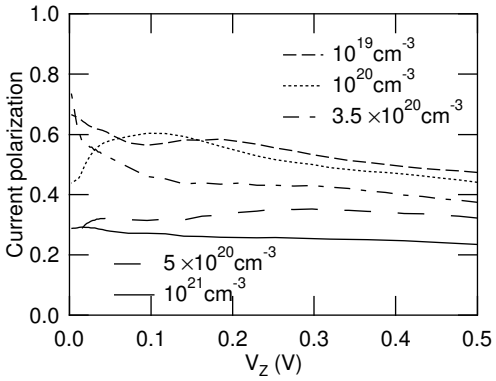

FIG. 6: The calculated bias dependence of the current polarization for different hole concentrations in the $Ga_{1-x}Mn_xAs$-layer for structure (a) of Fig. 5.

the spin-splitting. Surprisingly, however, a weak but opposite behavior is seen at low V_Z. We assign this result to the fact that the current polarization is determined not only by the electron spin polarization at the Fermi energy but also by the selection rules for transition probabilities. Actually, we know that the mixing of the spin wave functions, which reduces the tunneling matrix elements, is only important if the Fermi energy is much smaller than the spin-orbit splitting of the valence band. Accordingly, the reduction of P_j by the spin-orbit coupling decreases gradually with the hole density. Nevertheless, this effect appears to be too weak to explain much smaller P_j in the non-annealed sample from Ref. 4.

Next, to simulate more realistically the device, we consider the structure consisting of $Ga_{1-x}Mn_xAs$/GaAs/n-GaAs, where the GaAs spacer has to be kept thinner than that of the n-GaAs depleted layer implied by our self-consistent calculations. The schematic of such structure is shown in Fig. 5(b). Figure 7 shows P_j as a function of the bias V_Z of the Zener tunneling diode for various thicknesses d of the spacer layer. We see that at low bias, P_j depends weakly on d and is of the order of 0.7, in perfect agreement with the experimental results. Interestingly, the drop of P_j with V_Z, is greater for larger d. The strong dependence of P_j on V_Z is again in agreement with the experimental findings, though a direct comparison is hampered by the fact that the exact relation between V_Z and the total bias V applied to the device is unknown. The dependencies of P_j on V_Z and d can be easily explained with the help of Fig. 5(b), which shows that for $V_Z > 0$ the holes tunnel partly from the non-magnetic GaAs.

In conclusion, we have analyzed the spin polarization of the injected current in a (Ga,Mn)As-(Al,Ga)As spin-LED by performing self-consistent simulations of the band bending and using tight-binding model together with the Landauer-Buttiker formalism for the calculation of the tunneling current. Our studies explain quantitatively the large spin polarization of the injected current and its strong dependence on the applied voltage,

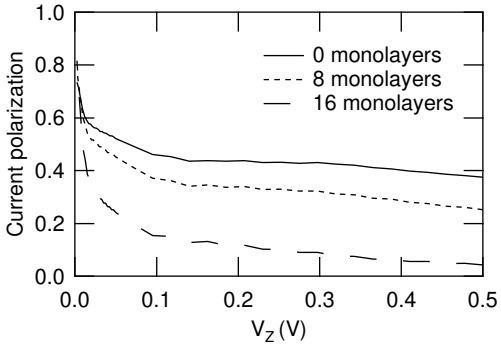

FIG. 7: The calculated bias dependence of the current polarization for different thicknesses of the spacer layer, for structure (b) of Fig. 5.

as has been recently observed in experiments. We ascribe the observed decrease of the spin polarization with the applied bias to the enhanced tunneling from depleted (Ga,Mn)As and non-magnetic GaAs regions. This can provide a path towards voltage controlled magnetic behavior. By choosing the right voltage drop over the tunnel diode, one can switch between injection from a magnetized region to injection from a non-magnetized region.

P.V.D. acknowledges financial support from the I.W.T. (Flanders), W.V.R. from the F.W.O. (Belgium), and P.S., P.K., and T.D. from the Polish Ministry of Science, Grant PBZ-KBN-044/P03/2001. This work is supported by the EC project FENIKS (G5RD-CT-2001-00535).

Electronic address: pvandorp@imec.be

[1] H. Ohno, J. Cryst. Growth 251, 285 (2003).

[2] M. Kohda, Y. Ohno, K. Takamura, F. Matsukura, and H. Ohno, Jpn. J. Appl. Phys. 40, L1274 (2001).

[3] E. Johnston-Halperin, D. Lofgreen, R. K. Kawakami, D. K. Young, L. Coldren, A. C. Gossard, and D. D. Awschalom, Phys. Rev. B 65, 041306 (2002).

[4] P. Van Dorpe, Z. Liu, W. Van Roy, V. F. Motsnyi, M. Sawicki, G. Borghs, and J. De Boeck, Appl. Phys. Lett. 84, 3495 (2004).

[5] For details, see: +http://www.synopsys.com+

[6] E. O. Kane, J. Phys. Chem. Solids 12, 181 (1959).

[7] T. Dietl, H. Ohno, and F. Matsukura, Phys. Rev. B 63, 195205 (2001).

[8] A. Di Carlo, Semicond. Sci. Technol. 18, R1 (2003), and the references therein.

[9] J.-M. Jancu, R. Scholz, F. Beltram, and F. Bassani, Phys. Rev. B 57, 6493 (1998).

[10] K. W. Edmonds, K. Y. Wang, R. P. Campion, A. C. Neumann, C. T. Foxon, B. L. Gallagher, and P. C. Main, Appl. Phys. Lett. 81, 3010 (2002).